



AN INVERSE LINEARIZATION MODEL FOR THE CHARACTERIZATION OF NON-CONTACT THERMOPILES

J-S. Botero V.¹ A. Salazar^{1,2} and L-J. Morantes G.¹

¹Grupo de investigación AEyCC,

¹Facultad de Ingenierías, Instituto Tecnológico Metropolitano ITM,
Carrera 31 No. 54-10, Medellín, Colombia.

²Grupo de Investigación SISTEMIC,

Facultad de Ingeniería, Universidad de Antioquia UdeA
Calle 70 No. 52-21, Medellín, Colombia

Email: juanbotero@itm.edu.co, luismorantes@itm.edu.co, augusto.salazar@udea.edu.co

Submitted: Dec. 16, 2015

Accepted: Mar. 20, 2016

Published: June 1, 2016

Abstract- A thermopile is an electronic device that converts thermal energy into electrical energy by means of arrangements of thermocouples that are connected in series. In addition, optical filters restrict the wavelength that strikes the thermopile. One of the main advantages of using a thermopile is its sensitivity to infrared radiation, which allows implementing non-contact thermometers. However, the thermopile does not provide an absolute temperature value, but a value that is proportional to the temperature gradient between the local temperature in the measurement range of the thermopile and its internal temperature. Therefore, it is necessary to integrate temperature sensors aiming to correct the output temperature value. In this sense, the output of the thermopile corresponds to a value generated from the relationship between the internal temperature of the thermopile and the output temperature. This work proposes and evaluates a thermopile characterization model, which uses an incubation system and a thermoelectric cooling device to control the room temperature and the temperature that is read out using the thermopile, respectively. This is based on the automation of the data collection procedure and the characterization of the thermistor that is used to measure the temperature of the thermopile. The result is an experimental operating surface, from which a linearization model was derived.

Index terms: Linearization, non-contact, thermopile, Peltier effect, thermistor.

I. INTRODUCTION

The thermopile is a passive thermal radiation detector that absorbs incoming radiation and converts it into an electrical signal, on the same principle as a thermocouple [1]. Usually it is built using arrays of thermocouples that are connected in series. Basically, it converts the difference between the ambient temperature and the temperature of the object being measured into a voltage using the Seebeck effect. This method is simple, requires no mechanics and can accurately detect static signals. A thermistor is used internally, which consists of a resistor that changes its resistance depending on the ambient temperature, to accurately measure the actual temperature [2]. It is a fact that at present the study of sensors and these networks is very important for IoT development and and reduce its cost [3]–[5].

The main applications of these sensors are non-contact temperature measurements and measurements of infrared radiation used in medical procedures [6]–[8], monitoring and process control [9]–[11], security systems [12], [13] and biological experiments [14] where the temperature is important. In [7] a thermopile array for detecting fever patients with infectious diseases in the clinical setting was developed. In [9] a calorimeter based on a thermopile was built for determining the heat output associated with the growth of microorganism cultures. In [11] a resonant inductive-capacitive (L-C) circuit-based wireless temperature sensor suitable for working in harsh environments to monitor the temperature of rotating components, such as jet turbines, engines, and power plants, etc. is presented. In [13] a technique is proposed to locate fire. The method is based on an arrangement of two thermopiles controlling an extinguisher system.

In order to ensure the reliability of those processes, i.e., that they operate within specified limits, calibration systems are utterly necessary, which is also important in measuring physical variables, e.g., for the properly estimation of the accelerometer's orientation [15], noise [5] or magnetometers [16]. The standard method for calibrating thermocouples by comparison techniques [17] is based on measuring the voltage of the sensor that is being analyzed at specific points, where the temperature at each point is being measured with a standard thermometer. The number and selection of the measurement points depend on the type of thermocouple, temperature range, and accuracy. In [18], they estimate that the calibration equations allow improving accuracy in two types of thermocouples by 0.4°C. In [19], they show calibration curves of two types of thermocouples, selecting five temperature ranks, to evaluate the fit with different polynomial

equations. Furthermore in [20], they characterized two different types of thermal sensors, thermistors and resistance temperature detectors, based on Labview's system interface to sensor, and associated an analog circuit for data conditioning, analysis, display, and control. However, despite that they are developed based on the same principle of measurement as infrared thermometers the literature does not report calibration studies of thermopiles.

A thermopile does not provide an absolute temperature value but one that is proportional to the temperature gradient between the local temperature in the measurement field of the thermopile and its internal temperature. Therefore, it is necessary to include temperature sensors to correct the output temperature value. This work proposes a characterization method based on a linearization procedure, which consists in the estimation of a function where the sensor output is the data set and the linearized response is the target of the estimation.

Adhering to the manufacturer's advice to use the data sheet, which suggests using look-up tables with steps of 10°C in different object temperatures and internal temperatures, leads to low accuracy. In this paper, a distribution function of temperature rise is generated for signal conditioning of thermopiles, which allows measuring a wide range of temperatures and has long-term stability and a high reliability.

The method proposed in this work can be used for the characterization of any thermopile. As a case study, we used a thermopile composed of 116 thermocouples. The temperature readings of an object were compared to those of a T type thermocouple in the controlled environment of an incubator at different ambient temperatures. Likewise, a thermoelectric cooling device based on the Peltier effect was used to vary the object's temperature and to generate a test surface to describe the behavior of the chosen sensor.

The main contributions of this work are:

- A method to compensate the effect of the room temperature on the read-out of a thermopile.
- An improving in the accuracy of the estimated temperature by replacing looking at a table of numbers from the manufacturer's data sheet for a surface that gives measures in a continuous manner within the whole range of measurement.
- For practical applications the calibration equation of the thermopile is expressed as an inverse equation.
- A characterization method that works for non-linear devices.

In addition to this introduction, the rest of this paper is organized as follows. The Section 2 describes the materials and methods used for the characterization of the sensor. Next, the experimental setup is depicted in Section 3. Section 4 shows the results of the proposed characterization method, and finally, the conclusions are drawn in Section 5.

II. MATERIALS AND METHODS

In this section we briefly describe the phenomena that define the behavior of the devices used in this work to derive the linearization model for the characterization of a thermopile.

First, we define the Seebeck Effect and the Peltier Effect, which are the cause of the thermoelectric effect [2], [21]. This phenomenon converts temperature differences at the junctions of two different conductors into voltage and vice versa.

a. The Seebeck and Peltier effects

The Seebeck Effect describes how a voltage is created from a temperature difference between two metals or semiconductors. This difference causes a current in the conductors, if they form a complete loop. Having two materials (A and B), the Seebeck potential is determined from the differential coefficient $\alpha_{AB} = \alpha_A - \alpha_B$ and the net voltage V_{AB} of the junction is given by

$$dV_{AB} = \alpha_{AB} dT .$$

The coefficient is temperature dependent, and therefore the potential is different at different temperatures [2].

The Peltier Effect refers to the reversible absorption of heat, when an electric current passes through a junction of two different metals. The effect occurs when power is applied externally or is induced by the thermocouple junction itself. The Peltier effect is used for two purposes: it can produce heat or cold (remove heat), depending on the direction of the current i , such as:

$$dQ_p = \pm p i dt .$$

The coefficient p has dimensions of voltage and represents the thermoelectric properties of the material [2].

Next, we describe the models used to estimate the temperature of an object using a combination of a thermistor and a thermopile.

b. Non-contact measuring of temperature

The resistance of a semiconductor can be modeled with the Steinhart-Hart model [22], described by Equation (1).

$$\frac{1}{T} = a + b \ln(R) + c (\ln(R))^3. \quad (1)$$

Where, T is the temperature in kelvin, R is the resistance of the semiconductor at T , and a , b , and c are the Steinhart–Hart coefficients. The value of the coefficients varies depending on the type of thermistor [2].

The β -model is a simplified version of the Steinhart-Hart equation with

$$a = \frac{1}{T_0} - \frac{1}{\beta} \ln(R_0), \quad b = \frac{1}{\beta}, \quad \text{and} \quad c = 0.$$

From above, the behavior of a thermistor can be described using the Equation (2).

$$\frac{1}{T} = \frac{1}{T_0} + \frac{1}{\beta} \ln\left(\frac{R}{R_0}\right), \quad (2)$$

where R_0 is the resistance at temperature T_0 (298.15 K). Typically, the values of R_0 and β are provided by the manufacturer, but we will demonstrate here that this values must be recomputed in order to get more accurate temperature values. From Equation (2), it is possible to define the resistance of a thermistor as a function of the temperature, thus,

$$R(T) = \tau e^{\frac{\beta}{T}}, \quad (3)$$

with

$$\tau = \frac{R_0}{e^{\frac{\beta}{T_0}}}.$$

Similarly, the temperature of a thermopile can be expressed as a function of the resistance as is described by Equation (4). This model was derived from Equation (3) and is used to compensate the polynomial model of a thermopile T_{TH} .

$$T_{TH}(R) = \frac{\beta}{\ln\left(\frac{R}{\tau}\right)}. \quad (4)$$

In the next section, we describe the devices used to characterize a non-contact temperature sensor. The OTP-538U thermopile and the TEC1-12706 thermoelectric cooler were selected as case of study, but the proposed method can be used for any other devices of the same kind. Also the incubator system controlling the room temperature, which was used as reference, is described.

c. Devices used in this work

Thermopile: The OTP-538U is a thermopile sensor composed of an array of 116 thermocouples in series on a floating membrane with a diameter of 545 microns and a dark surface to absorb incident infrared thermal radiation, which in response induces an electric tension in the terminal exits. The infrared (IR) window is a band pass filter with a 50% cut-on at a wavelength of 5 μm , and cut-down at 14 μm . The sensor responds proportionally to the impacting IR radiation and has a signal of constant response in its cut-off frequency, which is limited by the time constant. It also includes a thermistor with an earthed conductor that delivers the ambient temperature reference [23]. Table 1 shows the look-up table given by the manufacturer. As can be seen the measuring resolution is 10°C, which is very limited. We will demonstrate that, with the proposed calibration procedure,

the resolution is no longer limited even for a low cost device as the one used for the experiments carried out in this work.

Table 1. Typical Voltage Output Data (OTP-538U)

| Thermopile Output Voltage [mV] | | Thermistor Temperature [°C] | | | | | | | | | | | | |
|---|------|-----------------------------|-------|-------|-------|-------|-------|-------|-------|-------|-------|-------|-------|-------|
| | | -20 | -10 | 0 | 10 | 20 | 30 | 40 | 50 | 60 | 70 | 80 | 90 | 100 |
| Object Temperature [°C] | -20 | 0.00 | -0.25 | -0.52 | -0.83 | -1.18 | -1.56 | -1.98 | -2.45 | -2.96 | -3.52 | -4.13 | -4.79 | -5.51 |
| | -10 | 0.24 | 0.00 | -0.27 | -0.58 | -0.92 | -1.30 | -1.72 | -2.18 | -2.69 | -3.25 | -3.85 | -4.52 | -5.24 |
| | 0 | 0.51 | 0.27 | 0.00 | -0.30 | -0.64 | -1.02 | -1.43 | -1.89 | -2.40 | -2.95 | -3.56 | -4.22 | -4.93 |
| | 10 | 0.80 | 0.57 | 0.30 | 0.00 | -0.34 | -0.71 | -1.12 | -1.58 | -2.08 | -2.63 | -3.23 | -3.88 | -4.60 |
| | 20 | 1.13 | 0.89 | 0.63 | 0.33 | 0.00 | -0.37 | -0.78 | -1.23 | -1.73 | -2.27 | -2.87 | -3.52 | -4.23 |
| | 30 | 1.47 | 1.24 | 0.99 | 0.69 | 0.37 | 0.00 | -0.41 | -0.85 | -1.35 | -1.89 | -2.48 | -3.13 | -3.84 |
| | 40 | 1.85 | 1.63 | 1.37 | 1.08 | 0.76 | 0.40 | 0.00 | -0.44 | -0.93 | -1.47 | -2.06 | -2.70 | -3.40 |
| | 50 | 2.26 | 2.04 | 1.79 | 1.51 | 1.19 | 0.84 | 0.44 | 0.00 | -0.48 | -1.02 | -1.60 | -2.24 | -2.94 |
| | 60 | 2.71 | 2.49 | 2.25 | 1.97 | 1.66 | 1.30 | 0.91 | 0.48 | 0.00 | -0.53 | -1.11 | -1.74 | -2.43 |
| | 70 | 3.18 | 2.98 | 2.74 | 2.46 | 2.16 | 1.81 | 1.42 | 1.00 | 0.52 | 0.00 | -0.57 | -1.20 | -1.89 |
| | 80 | 3.70 | 3.50 | 3.26 | 2.99 | 2.69 | 2.35 | 1.97 | 1.55 | 1.08 | 0.57 | 0.00 | -0.62 | -1.30 |
| | 90 | 4.25 | 4.05 | 3.83 | 3.57 | 3.27 | 2.94 | 2.56 | 2.15 | 1.69 | 1.18 | 0.62 | 0.00 | -0.67 |
| | 100 | 4.84 | 4.65 | 4.43 | 4.18 | 3.89 | 3.56 | 3.20 | 2.79 | 2.33 | 1.83 | 1.28 | 0.67 | 0.00 |
| 110 | 5.47 | 5.29 | 5.08 | 4.83 | 4.55 | 4.23 | 3.87 | 3.47 | 3.02 | 2.53 | 1.98 | 1.38 | 0.72 | |

Thermoelectric cooler: The TEC1-12706 is a thermoelectric semiconductor cooling element based on the Peltier Effect. It creates a temperature difference that obtains low temperatures in a few minutes or heats up to 380 K by simply reversing the polarity. It is applied in CPU coolers and for cooling electronic components and small instruments. These devices should be used together with a heat sink, where one side is cooling and the other side is heating [24].

Incubator: we employ a device used for cell culture, where the humidity needs to be controlled. The device allows to vary the room temperature in a range between 278.15 K and 363.15 K. The systems has a capacity of 50 liters and holds a 50% of relative humidity. The reference temperature was measured with two T type thermocouples, which have an operation range from -250 °C to 400 °C, are NIST 175 standard compatible, and have a resolution of 0.1°C.

Finally, we explain how the distance from the target object to the sensor must satisfy a relationship proportional to the length of the object surface.

d. Measuring distance

As explained above, the sensor used contains internally an array of 116 thermocouples arranged in a membrane covered by an optical filter which responds above $4.7 \mu\text{m}$. Since this is a radiation measurement procedure, there exists a dependence on the distance between the object and the sensor and in addition also a dependence on the visual field of the thermopile, as shown in Figure 1.

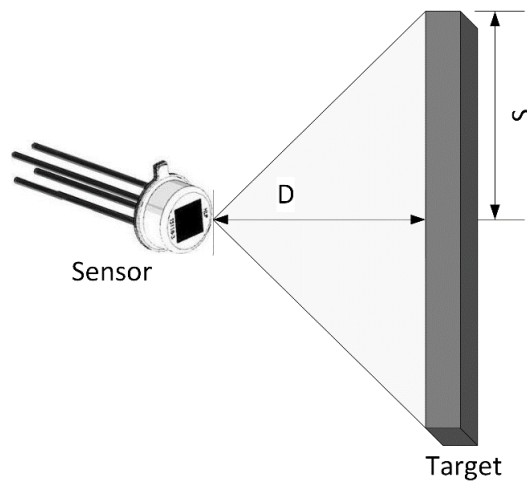


Figure 1. Thermopile distance

In the case of thermopile used in this work, the effective field of view can be considered 66° as the manufacturer suggests [14]. From this we can estimate the minimum distance at which the sensor should be arranged so that the measured surface covers the field of view of the thermopile, such as

$$D = S/\tan(33^\circ), \quad (5)$$

where D is the distance of the measured surface to the sensor and S is half the short side of the measured surface.

III. EXPERIMENTAL SETUP

Two different experiments were carried out in this work. First, we verified the theoretical model provided by the manufacturer of the thermistor. The second experiment aimed to generate a surface that captures the behavior of a thermopile as a function of its output voltage and the temperature of a target object, which is the basis of the inverse model introduced in this paper. In both experiments an incubator was used to guarantee a controlled room temperature. The reference temperature was measured with a T type thermocouple.

The validation of the theoretical model of the thermistor was compared with the one obtained from the interpolation of the resistance values, measured while varying the room temperature of the incubator in a range between 260 K and 360 K. A set of 100 samples was acquired, which corresponds to a sampling step of 1 K. By using Least Squares Minimization a curve was fitted to the data. As this curve corresponds to the theoretical model described by Equation (3), the experimental values of τ and β can be derived from the experimental data. This experiment is denoted as EC_T .

In order to model the relationship between the incident IR radiation and the internal temperature of a thermopile, read-outs in millivolts were obtained from the thermopile while the temperature of the Peltier cooler was varied. 15 different read-outs of the Peltier cell between 278.15 K and 363.15 K were taken, as well as 15 different ambient temperature values between 278.15 K and 363.15 K to obtain a total data set of 225 samples. This experiment is denoted as ES_{TH} . With these experimental data a surface was adjusted to a quadratic polynomial, as shown in Equation (6).

$$V = a_{00} + a_{10}T_{TH} + a_{01}T_{TP} + a_{20}T_{TH}^2 + a_{11}T_{TH}T_{TP} + a_{02}T_{TP}^2, \quad (6)$$

where T_{TP} and T_{TH} represent the temperatures of the Peltier cell (temperature of the target object) and the internal temperature of the thermopile, respectively. V corresponds to the voltage measured in the terminals of the thermopile. It is given that the value of V is known, thus T_{TH} is written in the form of a quadratic equation, as shown in Equation (7).

$$0 = a_{02}T_{TP}^2 + (a_{11}T_{TH} + a_{01})T_{TP} - (V + a_{00} + a_{10}T_{TH} + a_{20}T_{TH}^2). \quad (7)$$

Next, using the solution of a quadratic equation, Equation (7), which is defined as a function of V and T_{TH} , is solved. In this way, we introduce the calibration equation as an inverse equation, which is very useful in practice. Equation (8) shows the calibration equation of a thermopile.

$$T_{TP} = \frac{1}{2a_{02}} \left(-(a_{11}T_{TH} + a_{01}) + \left((a_{11}T_{TH} + a_{01})^2 + 4a_{02}(V + a_{00} + a_{10}T_{TH} + a_{20}T_{TH}^2) \right)^{1/2} \right). \quad (8)$$

Figure 2 depicts the configuration of the hardware used for the ES_{TH} experiment.

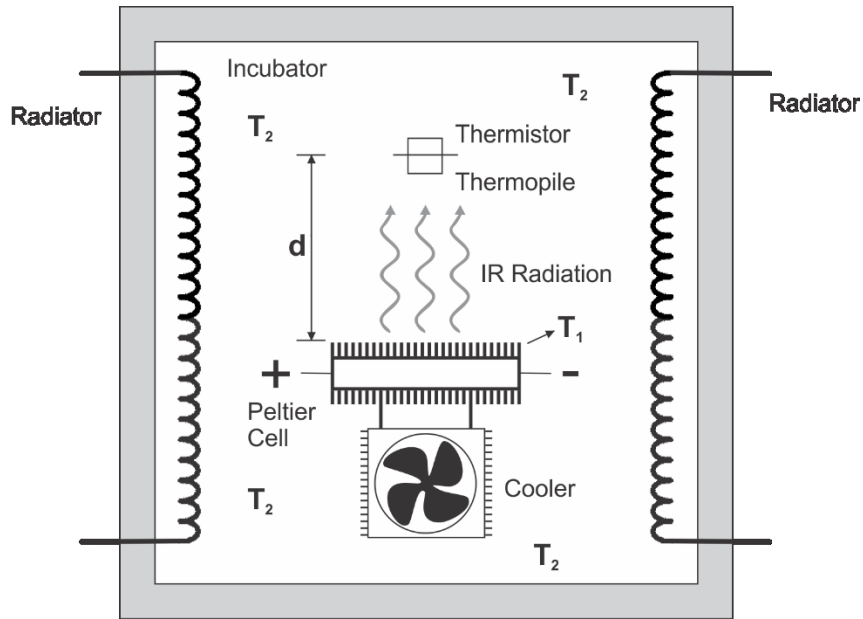


Figure 2: Hardware configuration for the ES_{TH} experiment. T_1 and T_2 correspond to the object and environment temperatures of reference, respectively.

IV. RESULTS

The results of the theoretical model and the experimental interpolation are shown in Figure 3. It has been observed that the theoretical model does not properly match the experimental behavior of the thermistor, which means that in order to obtain proper temperature readings, the calibration parameters have to be recomputed based on the curve generated from the interpolation of the experimentally collected data, as it has been explained in the description of the EC_T experiment.

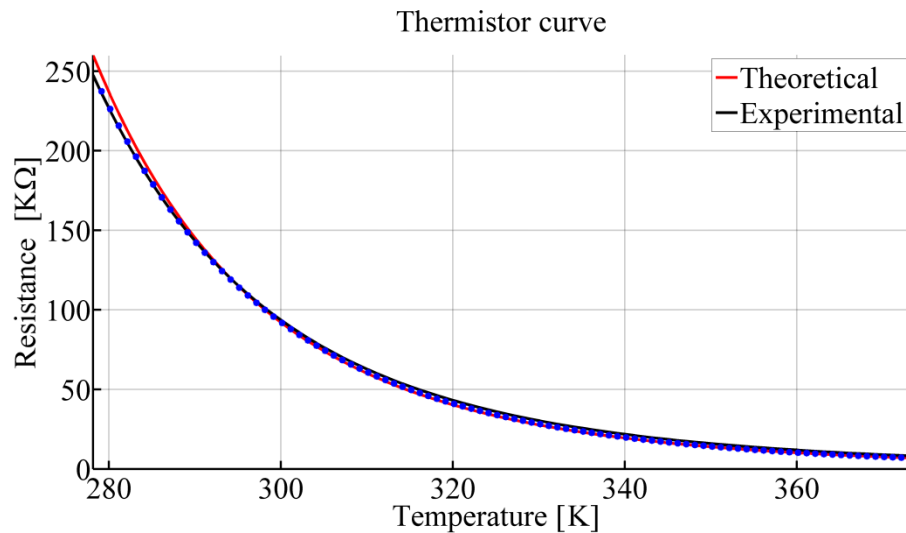


Figure 3: Comparison between theoretical and experimental thermistor curves.

Table 2 shows the parameters of the theoretical model in comparison to those obtained with the proposed experimental model. Notice the difference between the magnitudes of the parameters, which emphasizes the importance of the calibration procedures, as discussed before.

Table 2: Comparison of the theoretical and experimental model parameters

| | $R(298,15)$ [K] | τ | β |
|--------------|-----------------|----------|---------|
| Theoretical | 100 | 1,68E-04 | 3914 |
| Experimental | 101,05 | 3,92E-04 | 3715 |

Finally, Figure 4 shows the test surface describing the behavior of the thermopile. This surface was obtained from the data of the ES_{TH} experiment. Notice that the resolution of the measures is no longer limited to specific values, because it derived from a surface. In addition, for the first time, results were obtained from a model that combines the internal temperature of a thermopile, its output voltage, and the temperature of an object.

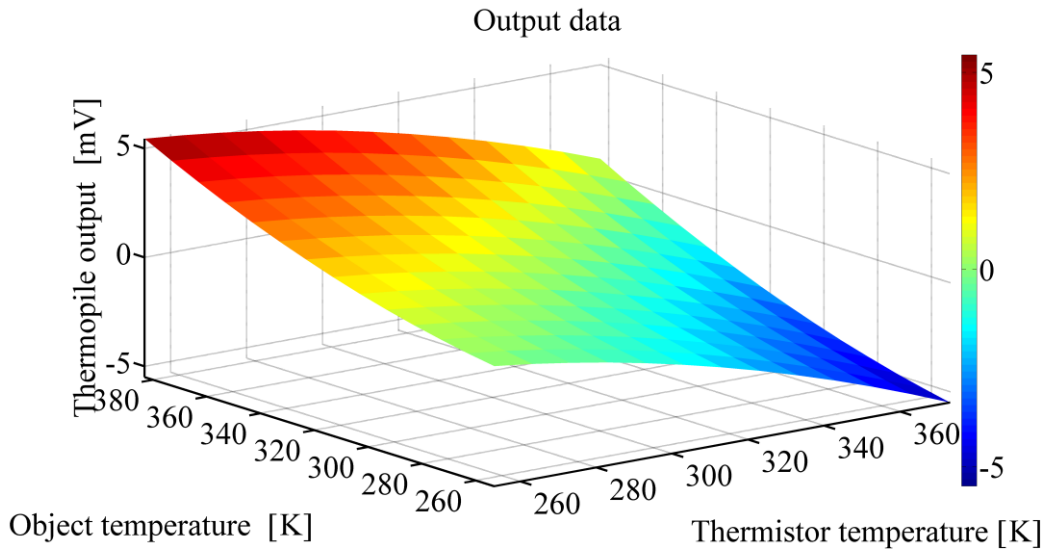


Figure 4: Thermopile surface

VI. CONCLUSIONS

A characterization method of a thermopile is proposed in this work. An incubation system controls the environmental temperature whereas a thermoelectric cooling device is used to vary the temperature of the object. The temperature measured with a T type thermocouple is used as a reference. With this setup, several readings are collected and a surface describing the behavior of the thermopile is derived. As a result, a calibration equation for thermopiles is proposed. This model allows obtaining more accurate read-outs in a broader temperature making the measurements more reliable.

As further work, we want to study the influence of the distance between the target object and the sensor, which results in a more compact model for non-invasive temperature measurement.

REFERENCES

- [1] T. M. Adams and R. A. Layton, *Introductory MEMS Fabrication and Applications*. Springer Science+Business Media, 2010.
- [2] J. Fraden, *Handbook of Modern Sensors: Physics, Designs, and Applications*, Fourth Ed. Springer New York, 2010.
- [3] M. Assaad, I. Yohannes, A. Bermak, D. Ginhac, and F. Meriaudeau, "Design and characterization of automated color sensor system," *Int. J. smart Sens. Intell. Syst.*, vol. 7, no. 1, pp. 1–12, 2014.
- [4] D. Bhattacharjee, G. Sharma, and R. Bera, "Universal intelligent sensor interface," *Int. J. Smart Sens. Intell. Syst.*, vol. 8, no. 4, pp. 2307–2327, 2015.
- [5] J. Hughes, J. Yan, and S. Kenichi, "Development of Wireless Sensor Network Using Bluetooth Low Energy (Ble) for Construction," *Int. J. Smart Sens. Intell. Syst.*, vol. 8, no. 2, pp. 1379–1405, 2015.
- [6] M. Liess, H. Karagözoglu, and H. Ernst, "Reducing thermal transient induced errors in thermopile sensors in ear thermometer applications," *Sensors Actuators A Phys.*, vol. 154, no. 1, pp. 1–6, Aug. 2009.
- [7] G. Sun, T. Saga, T. Shimizu, Y. Hakozaiki, and T. Matsui, "Fever screening of seasonal influenza patients using a cost-effective thermopile array with small pixels for close-range thermometry.," *Int. J. Infect. Dis. - IJID Off. Publ. Int. Soc. Infect. Dis.*, vol. 25, pp. 56–8, Aug. 2014.
- [8] A. Mahajan, C. Oesch, H. Padmanaban, L. Utterback, and F. Figueroa, "Physical and Virtual Intelligent Sensors for Integrated Health Management Systems," *Int. J. Smart Sens. Intell. Syst.*, vol. 5, no. 3, pp. 559–575, 2012.
- [9] J. Higuera-Guisset, J. Rodríguez-Viejo, M. Chacón, F. J. Muñoz, N. Vigués, and J. Mas, "Calorimetry of microbial growth using a thermopile based microreactor," *Thermochim. Acta*, vol. 427, no. 1–2, pp. 187–191, Mar. 2005.
- [10] S. a. O'Shaughnessy, M. a. Hebel, S. R. Evett, and P. D. Colaizzi, "Evaluation of a wireless infrared thermometer with a narrow field of view," *Comput. Electron. Agric.*, vol. 76, no. 1, pp. 59–68, Mar. 2011.
- [11] R. I. Rodriguez and Y. Jia, "A wireless inductive-capacitive (L-C) sensor for rotating component temperature monitoring," *Int. J. Smart Sens. Intell. Syst.*, vol. 4, no. 2, pp. 325–337, 2011.
- [12] K. Keränen, J.-T. Mäkinen, P. Korhonen, E. Juntunen, V. Heikkinen, and J. Mäkelä, "Infrared temperature sensor system for mobile devices," *Sensors Actuators A Phys.*, vol. 158, no. 1, pp. 161–167, Mar. 2010.
- [13] A. Pesatori and M. Norgia, "Infrared image system for fire location," *Measurement*, vol. 46, no. 10, pp. 4172–4178, Dec. 2013.
- [14] S. P. Singh and P. Singh, "Effect of temperature and light on the growth of algae species: A review," *Renew. Sustain. Energy Rev.*, vol. 50, pp. 431–444, 2015.
- [15] J.-S. Botero V., W. Hernandez, and E. Fernandez, "Orientation of a triaxial accelerometer using a homogeneous transformation matrix and Kalman filters," *Int. J. Smart Sens.*

- iIntelligent Syst.*, vol. 7, no. 4, pp. 1631–1646, 2014.
- [16] M. Kiani, S. H. Pourtakdoust, and A. A. Sheikhy, “Consistent calibration of magnetometers for nonlinear attitude determination,” *Measurement*, vol. 73, pp. 180–190, 2015.
- [17] ASTM International, “E220-13, Standard Test Method for Calibration of Thermocouples By Comparison Techniques,” in *Book of Standards*, West Conshohocken, PA: ASTM International, 2013.
- [18] C. Chen, Y.-K. Weng, and T.-C. Shen, “Performance evaluation of an infrared thermocouple,” *Sensors (Basel)*, vol. 10, no. 11, pp. 10081–94, Jan. 2010.
- [19] A. Chen and C. Chen, “Evaluation of piecewise polynomial equations for two types of thermocouples,” *Sensors (Basel)*, vol. 13, no. 12, pp. 17084–97, Jan. 2013.
- [20] N. Afsarimanesh and P. Z. Ahmed, “LabVIEW Based Characterization and Optimization of Thermal Sensors,” *Int. J. Smart Sens. Intell. Syst.*, vol. 4, no. 4, pp. 726–739, 2011.
- [21] X. C. Tong, *Advanced Materials for Thermal Management of Electronic Packaging*. Springer Science+Business Media, 2011.
- [22] J. S. Steinhart and S. R. Hart, “Calibration curves for thermistors,” *Deep Sea Res. Oceanogr. Abstr.*, vol. 15, no. 4, pp. 497–503, 1968.
- [23] Oriental System Technology Inc. - Orisystech, “Thermopile Sensor OTP-538U,” *Datasheet Oriental System Technology Inc.*, 2009. .
- [24] Hebei, “Thermoelectric Cooler TEC1-12 706,” *Datasheet Hebei I.T. (Shanghai) Co., Ltd.* .